



Defects interaction processes in deformed high purity polycrystalline molybdenum at elevated temperatures



O.A. Lambri^{a,*}, F.G. Bonifacich^a, P.B. Bozzano^b, G.I. Zelada^a, F. Plazaola^c, J.A. García^d

^a Laboratorio de Materiales, Escuela de Ingeniería Eléctrica, Centro de Tecnología e Investigación Eléctrica, Facultad de Ciencias Exactas, Ingeniería y Agrimensura, Universidad Nacional de Rosario – CONICET, Avda. Pellegrini 250, (2000) Rosario, Argentina

^b Laboratorio de Microscopía Electrónica, Unidad de Actividad Materiales, Centro Atómico Constituyentes, Comisión Nacional de Energía Atómica e Instituto Sábató – Universidad Nacional de San Martín, Avda. Gral. Paz 1499, (1650) San Martín, Argentina

^c Elekrika eta Elektronika Saila, Zientzia eta Teknologia Fakultatea, Euskal Herriko Unibertsitatea, P.K. 644, 48080 Bilbao, Spain

^d Departamento de Física Aplicada II, Facultad de Ciencias y Tecnología, Universidad del País Vasco, Apdo. 644, 48080 Bilbao, País Vasco, Spain

ARTICLE INFO

Article history:

Received 11 April 2014

Accepted 16 June 2014

Available online 23 June 2014

ABSTRACT

Mechanical spectroscopy (damping and elastic modulus as a function of temperature) and transmission electron microscopy studies have been performed in high purity polycrystalline molybdenum plastically deformed to different values of tensile and torsion strain. Mechanical spectroscopy measurements were performed from room temperature up to 1285 K. A relaxation peak in polycrystalline molybdenum related to the movement of dislocations into lower energy configurations near grain boundaries has been discovered to appear around 1170 K. The activation energy of the peak is $4.2 \text{ eV} \pm 0.5 \text{ eV}$. This relaxation phenomenon involves the interaction between vacancies and mobile dislocations near the grain boundaries. It should be highlighted that this relaxation process is controlled by the arrangement of vacancies and dislocations which occur at temperature below 1070 K.

© 2014 Elsevier B.V. All rights reserved.

1. Introduction

A broad range of alloys including austenitic stainless steels, ferritic–martensitic steels, refractory metals and titanium alloys have been investigated in extensive international materials testing programmes in order to identify potential candidates for the so-called first-wall region and other parts of a controlled thermonuclear reactor [1,2]. In particular, molybdenum has a high melting point, a high specific heat, good corrosion and creep resistance and strength at high temperatures. In addition, it has a relatively low thermal neutron cross section. These qualities make molybdenum attractive for the use in the nuclear industry [3]. Nuclear materials are exposed to irradiation and the same time to external stresses; therefore it is of great importance to understand the mechanisms of interaction between the defects into the material, in order to predict the long-time behaviour of these materials. Several works have been reported in the past 50 years about the mechanical properties in molybdenum and its associated recovery stages [4–14].

The temperature range around one third of the melting temperature ($0.3 T_m$, 865 K), usually related to stage V of recovery,

is particularly interesting in molybdenum due to the strong influence on the mechanical properties of both the pure metal and technological molybdenum-based alloys. In fact, in non-irradiated and irradiated molybdenum at annealing temperatures within stage V (temperatures higher than 850–900 K), the yield stress and the ultimate tensile strength begin to decrease [9,11,15].

Mechanical spectroscopy (MS), referred to as the internal friction method in the early literature, offers unique opportunities to study the mechanical energy losses due to the dislocation arrangement produced by deformation and its interaction with point defects [16].

The internal friction in molybdenum single crystals has been extensively discussed in the 50–1300 K temperature range, see for instance Benoit [17], Seeger [18], Zelada et al. [19–21] and Lambri et al. [22]. In particular, for temperatures higher than stage IV (600 K to 850–900 K) we reported that single crystalline deformed molybdenum exhibits two damping peaks. The physical mechanism which controls the damping peak appearing at around 700–800 K (so called the LTP) was related with the dragging of jogs by the dislocation under movement assisted by vacancy diffusion [19,20,22]. The damping peak which appears at high temperatures of around 950–1000 K (so called the HTP) was controlled by the formation and diffusion of vacancies assisted by the dislocation movement [20]. In addition, in plastically deformed and electron plus neutron irradiated high purity single crystalline molybdenum,

* Corresponding author. Tel.: +54 341 4802649/4802650x125; fax: +54 341 4821772/4802654.

E-mail address: olambri@fceia.unr.edu.ar (O.A. Lambri).

oriented for single slip, the intermediate temperature damping peak (so called the ITP) was detected at around 900 K. It was related to the interaction of dislocations lines with both prismatic loops and tangles of dislocation [21].

Nevertheless, little work is done on the internal friction of polycrystalline molybdenum above room temperature. Consequently, our aim is to study the mechanical energy losses in plastically deformed polycrystalline molybdenum from room temperature up to near 45% of the melting temperature (0.45 T_m). In addition, as it will be shown through the paper, the present results shed light on the physical driving force controlling the behaviour of the yield stress, ultimate tensile stress and ductile to brittle transition temperature in neutron irradiated molybdenum within the temperature range of stages IV and V of recovery during post-irradiation annealing.

2. Experimental

The samples used in this work were prepared from a single batch of “Amox Specialty Metals Corporation” low carbon arc cast 3/8” diameter rods in A.E.R.E, Harwell, UK. The specifications of this starting material were: C 0.004%, O₂ 0.0004%, H₂ 0.0001%, N₂ 0.0001%, Fe 0.002%, Ni 0.001% and Si 0.002%. Samples were decarburized for 48 h by heating them, using an R.F. induction furnace, to 1873 K in a partial pressure 8×10^{-3} Pa of oxygen. The oxygen atmosphere was maintained by continuously bleeding spectroscopically pure oxygen through a leak valve. The carbon removal was monitored by the amounts of CO and CO₂ in the residual vacuum by using a mass spectrometer. After the decarburization process the samples were annealed at 2073 K for 24 h in a vacuum better than 10^{-5} Pa to remove the oxygen.

The average grain size was 50 μm. No appreciable change in grain size could be detected after the heat treatments during the performed measurements in the present work. The samples were sheets of 20 mm length, 0.4 mm thickness and 2.5 mm width.

Samples were deformed in tensile at a constant speed of 0.03 cm/min, followed by 1.5% torsion at room temperature.

Damping, Q^{-1} (or internal friction), and natural frequency were measured in an inverted torsion pendulum, under a vacuum of about 10^{-5} Pa. The maximum strain on the surface of the sample was 5×10^{-5} . The measurement frequency was around 1 Hz except in the determination of the frequency dependence of the peak temperature. The heating and cooling rates employed in the tests were of 1 K/min. A heating and its corresponding cooling run will be called hereafter a thermal cycle. There was no hold time once the maximum temperature had been achieved, during the thermal cycle.

During the run -up and -down in temperature, Q^{-1} was calculated from the slope of the straight line which results from the least squares fitting of the natural logarithm of all the decaying amplitudes versus time, such that

$$\ln(A_n) = \ln(A_0) - \pi Q^{-1} n \quad (1)$$

where A_n is the area of the n th decaying oscillation, A_0 is the initial area of the starting decaying oscillation and n is the period number. For all these measurements the same initial and end values of the decaying amplitudes were used for eliminating some possible distortion for the appearance of amplitude dependent damping effects [23].

Amplitude dependent damping (ADD), i.e. damping as a function of the maximum strain on the sample, ϵ_0 , was calculated from Eq. (2) [19,23,24]

$$Q^{-1}(\epsilon_0) = -\frac{1}{\pi} \frac{d(\ln(A_n))}{dn} \quad (2)$$

The decaying of the oscillations were performed at constant temperature ($T \pm 0.5$ K). Polynomials were fitted to the curve of the decaying areas of the torsional vibrations as a function of the period number by means of Chi-square fitting. Subsequently the Eq. (2) was applied. Polynomials of degree higher than 1 indicate that Q^{-1} is a function of ϵ_0 , leading to the appearance of ADD effects, as it can be inferred easily. This procedure allows obtaining the damping as a function of the maximum strain (ϵ_0) from free decaying oscillations [19,23,24]. The degree of fitted polynomials was smaller than 3.

The strength of ADD effects is measured through S parameter, such that [19,23,24].

$$S = \frac{\Delta Q^{-1}}{\Delta \epsilon_0} \quad (3)$$

For transmission electron microscopy (TEM) examinations, thin foils were prepared with the double jet technique using 12% H₂SO₄ in methyl alcohol. Observations were carried out in a Phillips CM200 transmission electron microscope operated at 200 kV.

3. Results

3.1. Mechanical spectroscopy

Fig. 1 shows the damping spectra measured from 800 K up to 1285 K, for a polycrystalline sample deformed 1% in tensile and 1.5% in torsion at room temperature. Full symbols are for heating runs and the corresponding empty ones, are for cooling. In the first run up to 1240 K (full rhombus in the figure) the samples showed an increasing background with temperature. Nevertheless, on cooling a small damping hump around 1170 K appears. For the next heating run a step like damping is seen at this temperature (squares in the figure). During the following heating run (full circles) a damping peak develops which is clearly observed at 1170 K, but during cooling the peak disappears. In the following runs, for thermal cycles from room temperature up to 1285 K the peak stabilizes at around 1170 K (for the last spectrum, triangles, only the heating run is shown), but it is always absent during the cooling part of the cycles. The HTP appearing in single crystals cannot be clearly observed, although a hump around 950 K is present in the spectra which presents the damping peak at 1170 K, see full circles and triangles in Fig. 1.

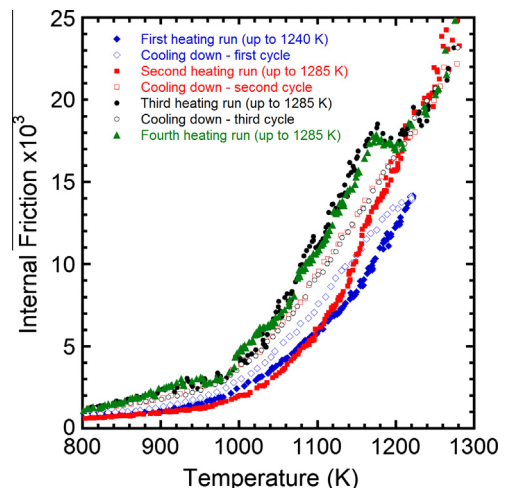


Fig. 1. Damping spectra measured during successive thermal cycles for a polycrystalline molybdenum sample deformed 1% in tensile and 1.5% in torsion at room temperature. Full symbols: heating part of thermal cycle. Empty symbols: cooling part of thermal cycle.

In the other hand, annealed samples present an increasing background with temperature in the heating and cooling runs, but do not show any damping peak.

Fig. 2 shows the internal friction spectra in Fig. 1, but for the 300–900 K temperature range. The most prominent feature is that for cooling runs which did not present the peak at 1170 K (empty squares and circles in Fig. 1) they show, in this temperature range, a damping peak between 500 K and 600 K, see empty squares and circles in Fig. 2. These peaks do not appear during the corresponding heating runs; see full symbols in Fig. 2.

This low temperature peak appears at lower temperature than the LTP in single crystals and its behaviour is different. The LTP was present in the heating and cooling runs [19,20,22], while the peak in the present polycrystalline samples, as said before, only appears in the cooling runs when the peak at 1170 K disappears.

Fig. 3 shows the moduli (square of frequency) in the temperature range 300–1285 K, which correspond to the spectra in Figs. 1 and 2. The square of the frequency decreases as the temperature increases and presents slope changes at temperatures corresponding to those of the internal friction peaks at 500–600 K and 1170 K. In the last cooling run presented in the figure (empty circles) there is a noticeable modulus increase at the temperature where the internal friction peak at around 500 K appears. Spectra, also present an important drop at around 1070 K which means that the modulus of the sample decreases noticeably for temperatures higher than 1070 K.

Fig. 4 shows the damping spectra measured from 800 K up to 1285 K, for a polycrystalline sample deformed 5% in tensile and 1.5% in torsion at room temperature. Full symbols are for heating and the corresponding empties ones, are for cooling. The first heating run, up to 1285 K (rhombus) shows an increasing damping with temperature. For the following runs (squares and circles) the damping values grow, presenting a clear step like increase above 1150 K. Damping values are almost ten times higher than the ones measured in 1% deformed samples, see Fig. 1. The difference in the damping values between the samples deformed 1% and 5%, becomes more evident for temperatures higher than 1150 K. In this case, for 5% deformed samples, the damping peak at 1170 K cannot be clearly distinguished from the high internal friction background.

The square of the frequency in the temperature range 300–1285 K, which correspond to spectra in Fig. 4, are shown in Fig. 5. This figure shows that the square of the frequency presents an important drop at around 1070 K which means that the

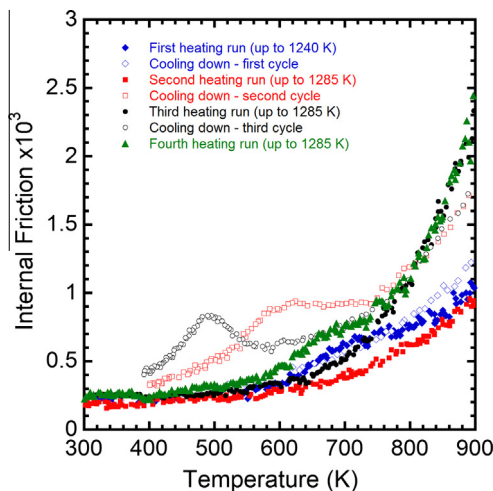


Fig. 2. Damping spectra in Fig. 1, but for the 300–900 K temperature range. Symbols mean as in Fig. 1.

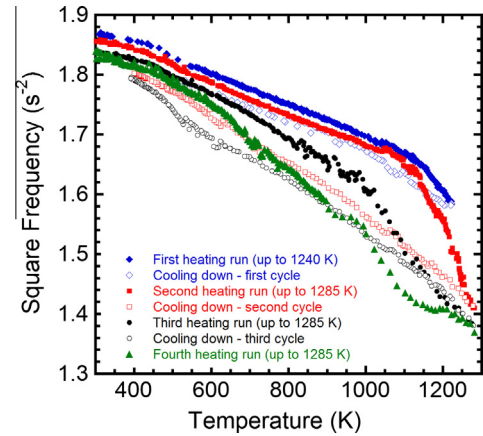


Fig. 3. Square of frequency (proportional to elastic shear modulus) curves corresponding to spectra in Figs. 1 and 2. Full symbols: heating part of thermal cycle. Empty symbols: cooling part of thermal cycle.

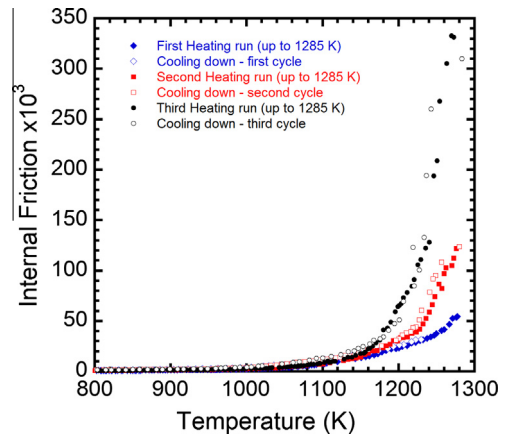


Fig. 4. Damping spectra measured during successive thermal cycles from 800 K up to 1285 K, for a polycrystalline sample deformed 5% in tensile and 1.5% in torsion at room temperature. Full symbols: heating part of thermal cycle. Empty symbols: cooling part of thermal cycle.

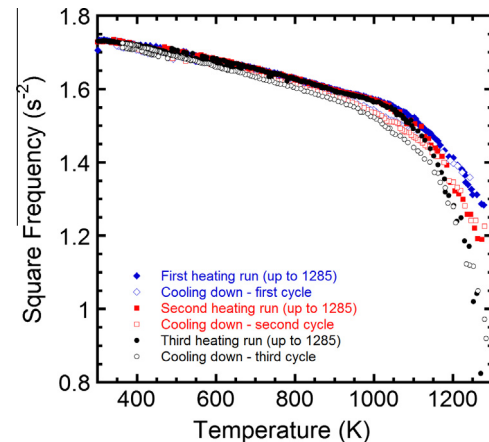


Fig. 5. Square of frequency (proportional to elastic shear modulus) curves corresponding to spectra in Fig. 4. Full symbols: heating part of thermal cycle. Empty symbols: cooling part of thermal cycle.

modulus of the sample decreases noticeably for temperatures higher than 1070 K. This behaviour is similar, but more intense, to the one exhibited by the samples deformed 1%.

Fig. 6 shows the behaviour of the S parameter during the successive thermal cycles for the sample deformed 1% in tensile and 1.5% in torsion, at room temperature, in Fig. 1. S curve for the third thermal cycle was not plotted for the sake of clarity, but it almost overlaps on curve for the fourth thermal cycle. S values for samples stretched 2% and 5% increase as the deformation degree increases, but the whole trends are similar than those for the sample deformed 1%.

3.2. Transmission electron microscopy

Fig. 7 shows the dislocation arrangement resulting after room temperature plastic deformation, 1% tensile plus 1.5% torsion, in polycrystalline molybdenum. As it can be observed deformation give rise to a heterogeneous pattern of dislocations, where dislocations appear very tangled in some zones and in addition, a lot of short and rough dislocations develop.

In Fig. 8a, a bright field micrograph of a grain boundary with dislocations near it, can be seen. The dark field, Fig. 8b, reveals clearly dislocations segments in one grain and dislocations agglomerated near the grain boundary. Fig. 8b was obtained by the (2, -1, 1) reflection of the selected area diffraction pattern (Fig. 8c and d).

Fig. 9a and b shows zones with tangles of dislocations and planar arrays of dislocations, respectively, for a sample deformed plastically 1% tensile plus 1.5% torsion, after performing the thermal cycles in the mechanical spectrometer.

As it can be seen from the micrographs Fig. 9a and b the dislocation structure is re-arranged after the successive thermal cycles in the spectrometer, leading to a configuration of less entangled dislocations. In addition, a high magnification image of the upper left zone of Fig. 9b is shown in Fig. 9c and d. Fig. 9c (bright field) and d (dark field) show a dislocation wall, probably due to the recovery process, where dislocations move from a tangled orientation to form a sub-boundary during the annealing at high temperatures [25,26]. The movement of dislocations into this lower energy configuration is part of the recovery process.

4. Discussion

The modulus drop in Figs. 3 and 5 shows that around 1070 K the sample suffers a softening due to the increased mobility of the dislocations produced by deformation. This is also revealed by the marked increase both in the internal friction background (see Figs. 1 and 4) and S values (see Fig. 6), from this temperature

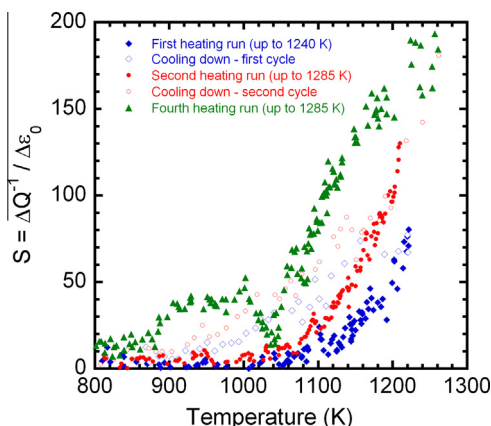


Fig. 6. $S = \Delta Q^{-1}/\Delta \epsilon_0$ as a function of temperature during successive thermal cycles for a polycrystalline molybdenum sample deformed 1% in tensile and 1.5% in torsion at room temperature. Full symbols: heating part of thermal cycle. Empty symbols: cooling part of thermal cycle.

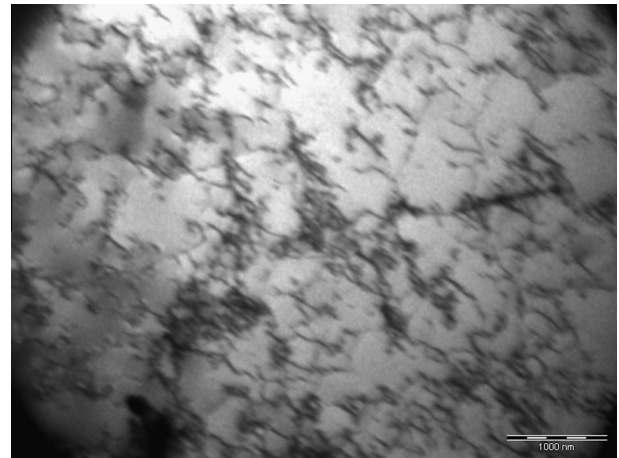


Fig. 7. TEM micrograph for polycrystalline molybdenum after room temperature plastic deformation, 1% tensile plus 1.5% torsion.

onwards. Taking this into account, the internal friction of the sample was measured by cycling in temperature only down to 1070 K, instead of decreasing the temperature in the cooling run down to room temperature as in the previous thermal cycles. Fig. 10 shows the damping for the last heating run presented in Fig. 1 (full triangles). In the subsequent cooling run from 1285 K the sample was only cooled up to 1070 K (empty triangles in Figure). In the next heating run from this temperature (full squares) the damping peak at 1170 K was not present. This indicates that the peak has to be related to a process occurring at temperatures below 1070 K.

The activation energy of the peak at 1170 K was measured for samples deformed 1% in tensile and 1.5% in torsion. Fig. 11 shows the Arrhenius plot (the frequency dependence of the peak temperature, T_p) [16] for the measured values at three different frequencies 0.8 Hz, 1.4 Hz and 7 Hz, see Section 2. Inset in Fig. 11 shows the damping peaks after the background subtraction for the different oscillating frequencies. Damping background subtraction was done by using cubic polynomials through Peak Fit V.4 soft [27].

The activation energy, H , obtained from the plot is $4.2 \text{ eV} \pm 0.5 \text{ eV}$. This activation energy is higher than the ones obtained in single crystalline molybdenum for the LTP, ITP and HTP, which were 1.6 eV, 1.9 eV and 2.7 eV; respectively. In addition, the activation energy related to the present work, damping peak at 1170 K in plastically deformed polycrystalline samples, is very close to the self diffusion energy for molybdenum, $\approx 4.5 \text{ eV}$ [28,29].

Taking into account that the peak is developed in plastically deformed samples and that the peak is not resolved in annealed samples, the peak has to be related to a relaxation process involving dislocations. In addition, the peak was not present in single crystalline samples [19–22] and, besides, the temperature range where the peak appears, near $0.4 T_m$ (1170 K), is the expected temperature range for the grain boundary peak [16,30,31]. Consequently, this damping peak can be related to the movement of dislocations into lower energy configurations near grain boundaries.

ADD experiments, also confirm this point, see Fig. 6. In fact, the strong increase in S values indicates that a larger mobility of dislocations starts at temperatures where the 1170 K peak begins to be developed, see inset in Fig. 11, in agreement with the above exposed. Besides, from TEM micrographs, it is evident the reorganization of the dislocation arrangements after annealing during the thermal cycles, see Figs. 7–9.

Moreover, the peak temperature depends on the degree of plastic deformation, as it is shown in Fig. 12. Despite the background

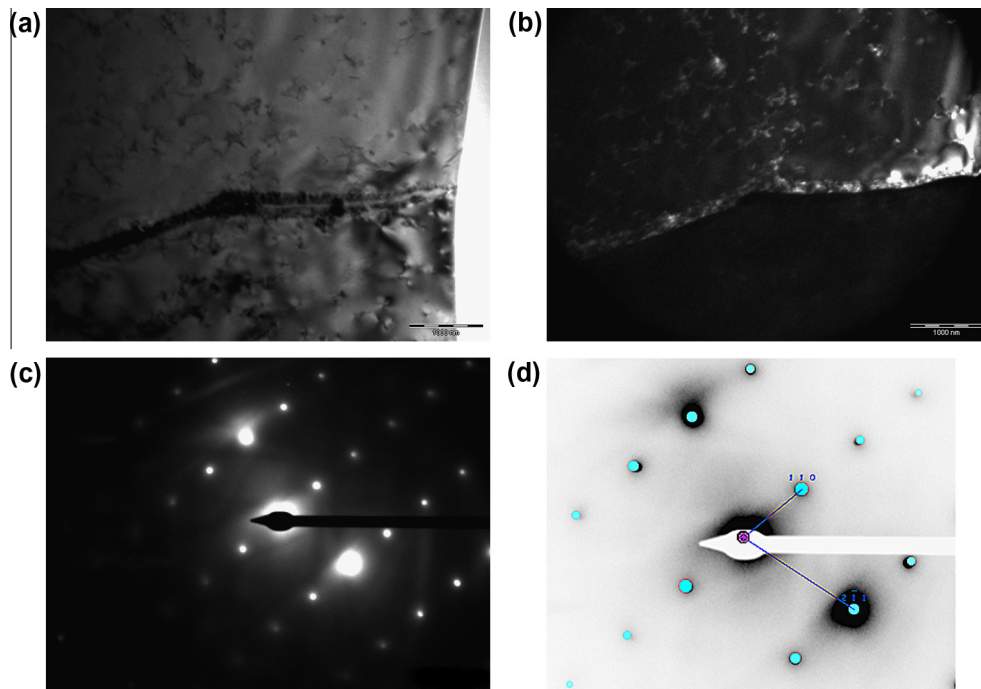


Fig. 8. (a) Bright field in polycrystalline molybdenum after room temperature plastic deformation, 1% tensile plus 1.5% torsion. Note the presence of a dislocation arrange near the grain boundary. (b) Corresponding dark field, obtained from one diffracted spot reported in (c). As can be seen only one grain is in the Bragg position. (d) Selected area diffraction pattern and its corresponding explanatory diagram (Zone Axis [001]).

subtraction could not be realized due to the high internal friction values, the displacement of the peak maximum can be clearly observed. Fig. 12 shows the position of the peak for three different tensile deformations 1%, 2% and 5% plus an additional 1.5% in torsion in all the cases. The scale of the internal friction is logarithmic and the position of the damping peak is indicated by means of arrows. It can be seen that the higher the tensile deformation, the higher is the temperature where the peak appears. This indicates that when the density of dislocation increases, dislocations and also sub-boundaries near grain boundaries are more entangled leading to a shift of the peak to higher temperatures. In addition, as said before, the appearance of ADD effects within the range of the peak temperature at 1170 K, see Fig. 6, clearly indicates that the relaxation at 1170 K involves the movement of dislocations and sub-boundaries near grain boundaries.

Furthermore, it should be pointed out that the damping peak at 1170 K has to be related to the processes that dislocations suffer at temperatures below 1070 K, because the peak does not appear in the warming run if the sample is not cooled below 1070 K.

As it was shown (see Fig. 1), the peak is present during the heating, but it is absent during the subsequent cooling. This, can be due to the rearrangement of the dislocation structure after the annealing at 1285 K. Deformed structure recovers after annealing to 1285 K in order to decrease its free energy, in agreement with the recrystallization temperature reported for molybdenum, 1173 K [3]. Even, if only a partial recrystallization occurs, since the grain size does not change clearly, both damping and modulus curves show a clear recovery. It is revealed by the decrease in the modulus and the increase in the damping values (see Figs. 1 and 3–5) in agreement with the less tangled arrangement of dislocations after thermal cycles performed at the pendulum (see Fig. 9a and b). This process leads to a rearrangement of defects in polycrystalline molybdenum which will inhibit the appearance of the peak at 1070 K during the cooling.

The absence of the peak at 1070 K during the cooling has to be related also to the appearance, at the same time, of the damping

peak at around 500–600 K, see Figs. 1 and 2. Pinning of dislocations by vacancies was reported to appear within the temperature interval 400–700 K [32]. Moreover, vacancies in molybdenum tend to agglomerate at around 550 K [33], so during the cooling vacancies could agglomerate around that temperature, interacting with the dislocations arrangement through a pinning process giving rise to the damping peak at around 500 K. In a subsequent heating run, dislocations are already pinned by vacancies agglomerates and then the damping peak at around 500 K does not appear.

When the temperature increases, vacancy agglomerates dissolve and vacancies migrate to the dislocations and grain boundaries easing, at around 1070 K, the mobility of the dislocations near the grain boundaries and giving rise to the appearance of the peak at 1170 K. In fact, this mechanism is in agreement with the activation energy calculated for this process $4.2 \text{ eV} \pm 0.5 \text{ eV}$ which corresponds to a value for self diffusion, indicating a process of vacancy motion to dislocations.

The interaction mechanism between vacancies and dislocations, within the temperature range of stage V, described in this work is important in order to understand the behaviour of the mechanical properties of polycrystalline molybdenum at temperatures within this stage. Wrosny and Johnson [9] reported that neutron irradiated polycrystalline molybdenum at 313 K followed by annealing at temperatures over 400 K lead to an increase in the yield stress and in the ultimate tensile strength (UTS). This behaviour was attributed to the diffusion of vacancies produced by irradiation towards the lattice sinks during the annealing process, leading to the promotion of vacancy clusters which increase the frictional stresses in the lattice [9]. Cockeram et al. [15] explained the increase in temperature of the ductile to brittle transition temperature (DBTT) in neutron irradiated samples, on the basis that diffusion rate of point defects in molybdenum was slow enough at temperatures less than 1073 K. That leads to the nucleation of a fine dispersions of voids and dislocations loops produced by irradiation, giving rise to a decrease in the dislocation mobility [15].

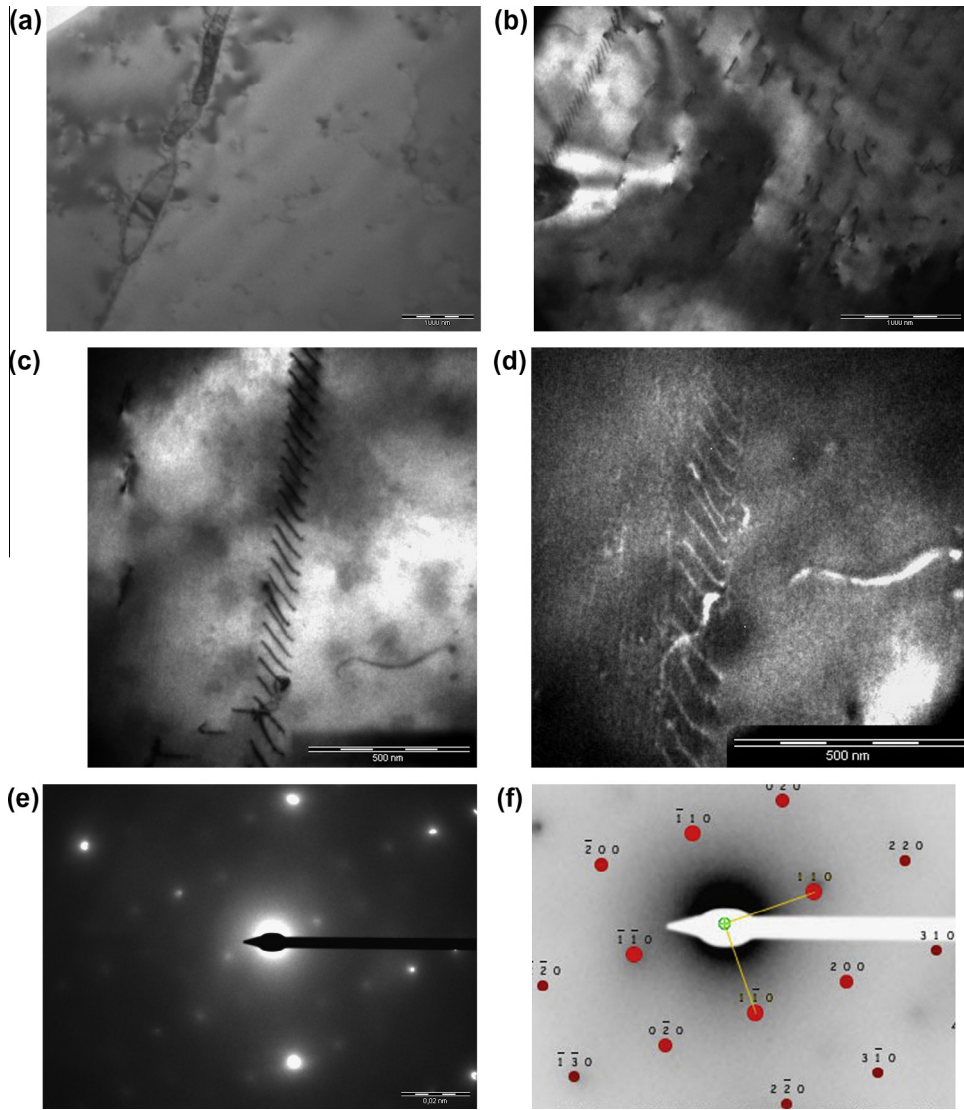


Fig. 9. (a and b) TEM micrographs for room temperature plastically deformed polycrystalline molybdenum (1% tensile plus 1.5% torsion) after performing the thermal cycles in the mechanical spectrometer. (c and d) High magnification images of the upper left zone of (b). (c) Dislocation wall (bright field). (d) Dark field of the zone (e). (f) Selected area diffraction pattern and its explanatory diagram (Zone Axis [001]).

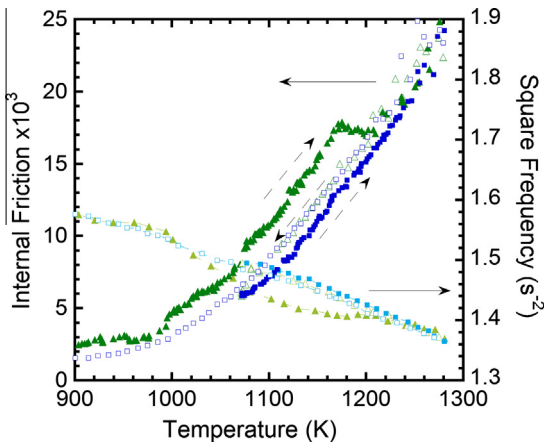


Fig. 10. MS spectra measured during thermal cycles, but with cooling down to 1070 K. Full symbols: heating part of thermal cycle. Empty symbols: cooling part of thermal cycle. Broken arrows indicate the heating and cooling parts.

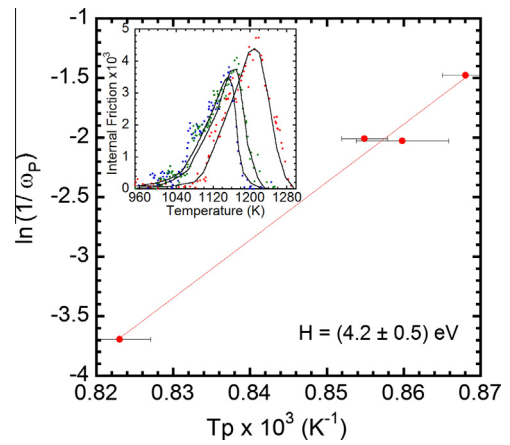


Fig. 11. Arrhenius plot for the peak at 1170 K. T_p : Peak temperature. ω_p : Circular frequency at the peak temperature. Inset: damping peaks after the background subtraction for the different oscillating frequencies, see explanation in the text.

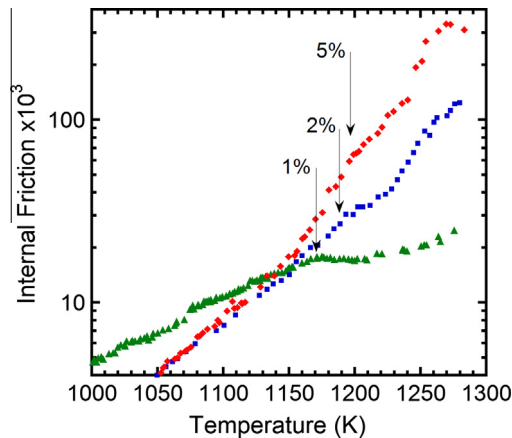


Fig. 12. Damping spectra measured during the heating part of thermal cycles for samples stretched at different degree. Torsion: 1.5% in all the cases. Triangles: 1%, squares: 2%, rhombus: 5%. Arrows indicate the approximate temperature of peak.

In the present work we show that in polycrystalline molybdenum the damping mechanism of the peak at 1170 K is related to a process occurring when most of the excess of vacancies produced by plastic deformation are removed by annihilation at dislocations to produce recovery by the movement of dislocations into lower energy configurations. Remember that the peak starts to develop after the thermal cycle anneals the sample up to 1223 K, see rhombus in Fig. 1, and in molybdenum the excess of vacancies promoted by neutron irradiation recover markedly after annealing at temperatures over 1000 K [33]. Then, it can be proposed that in polycrystalline molybdenum the behaviour of the yield stress, UTS and DBTT could be controlled by the interaction process between clusters of vacancies and dislocations, where the larger dislocation contribution corresponds to dislocations located at the grain boundaries.

5. Conclusion

A damping peak in high purity polycrystalline molybdenum related to the movement of dislocations into lower energy configurations near grain boundaries has been discovered to appear around 1170 K. It should be highlighted that this relaxation process is controlled by the arrangement of vacancies and dislocations which occur at temperature below 1070 K. This is revealed by the fact that the appearance of the peak at 1170 K, is conditioned to the cooling of the sample below 1070 K. Vacancies agglomerates interacting with dislocations at temperatures below 1070 K are required to promote the relaxation process at 1170 K. The activation energy of the peak for this process is $4.2 \text{ eV} \pm 0.5 \text{ eV}$.

Acknowledgements

We acknowledge to Prof. J.N. Lomer for the polycrystalline samples, to Prof. M. Ipohorski for his invaluable contribution on TEM discussing, to B.A. Pentke for the preparation of samples for TEM and G.M. Zbihlei for the technical support during the TEM observations. This work was partially supported by the Collaboration Agreement between the Universidad del País Vasco and the Universidad Nacional de Rosario: Res. CS.788/88 – 1792/2003, UPV224.310-14553/02, Res. 3469/2007 and Res. CS. 124/2010 (2009–2014), the CONICET-PIP 2098 and 0179, and the PID-UNR; ING 290 (2010–2013) and 453 (2014–2017).

References

- [1] J. Mazey, C.A. English, *J. Less Com. Metals* 100 (1984) 385–427.
- [2] C. Cabet, J. Jang, J. Konys, P.F. Tortorelli, *MRS Bull.* 34 (2009) 35–39.
- [3] S. Nemat-Nasser, W. Guo, M. Liu, *Scr. Mater.* 40 (1999) 859–872.
- [4] B. Mastel, L. Brimhall, *Acta Metall.* 13 (1965) 1109–1116.
- [5] L. Brimhall, B. Mastel, T.K. Bierlein, *Acta Metall.* 16 (1968) 781–788.
- [6] R.C. Rau, J. Mottef, R.L. Ladd, *J. Nucl. Mater.* 40 (1971) 233–235.
- [7] C.C. Matthai, D.J. Bacon, *J. Nucl. Mater.* 125 (1984) 138–151.
- [8] J. Cornelis, P. de Meester, L. Stals, J. Nihoul, *Phys. Status Solidi (a)* 18 (1973) 515–522.
- [9] A.S. Wrotsky, A.A. Johnson, *Phil. Mag.* 213 (1963) 1067–1070.
- [10] H.B. Afman, *Phys. Status Solidi (a)* 13 (1972) 623–630.
- [11] J. Nihoul, *Symp. on Radiation Damage in Solids and Reactor Materials*, vol. I, IAEA, Vienna 1962, SM 25.
- [12] G.L. Kulcinsky, H.E. Kissinger, *Phys. Status Solidi (a)* 2 (1970) 267–272.
- [13] A.A. Johnson, *J. Less Com. Metals* 2 (1960) 241–252.
- [14] B.V. Cockeram, J.L. Hollembeck, L.L. Snead, *J. Nucl. Mater.* 324 (2004) 77–89.
- [15] B.V. Cockeram, J.L. Hollembeck, L.L. Snead, *J. Nucl. Mater.* 336 (2005) 299–313.
- [16] R. Schaller, G. Fantozzi, G. Gremaud (Eds.), *Mechanical Spectroscopy*, Trans. Tech. Publ. Ltd, Switzerland, 2001.
- [17] W. Benoit, *Dislocation relaxations*, in: R. Schaller, G. Fantozzi, G. Gremaud (Eds.), *Mechanical Spectroscopy*, Trans. Tech. Publ. Ltd, Switzerland, 2001, pp. 141–177.
- [18] A. Seeger, *Phil. Mag. Lett.* 83 (2003) 107–115.
- [19] G.I. Zelada-Lambri, O.A. Lambri, J.A. García, *J. Nucl. Mater.* 353 (2006) 127–134.
- [20] G.I. Zelada-Lambri, O.A. Lambri, P.B. Bozzano, J.A. García, C.A. Celauro, *J. Nucl. Mater.* 380 (2008) 111–119.
- [21] G.I. Zelada, O.A. Lambri, P.B. Bozzano, J.A. García, *Phys. Status Solidi A* 209 (2012) 1972–1977.
- [22] O.A. Lambri, G.I. Zelada-Lambri, L.M. Salvatierra, J.A. García, J.N. Lomer, *Mater. Sci. Eng. A* 370 (2004) 222–224.
- [23] O.A. Lambri, A review on the problem of measuring nonlinear damping and the obtainment of intrinsic damping, in: Wörner, Walgraef (Ed.), *Martinez-Mardones, Materials Instabilities*, New York, 2000, pp. 249–280.
- [24] B.J. Molinas, O.A. Lambri, M. Weller, *J. Alloys Compd.* 211–212 (1994) 181–184.
- [25] F.J. Humphreys, M. Hatherly, *Recrystallization and Related Annealing Phenomena*, Pergamon/Elsevier Science, The Netherlands, 2002.
- [26] R.W. Cahn, P. Haasen, *Physical Metallurgy*, North-Holland, Amsterdam, 1983.
- [27] *Peak Fit, V. 4*, Jandel Scientific Software, Germany, 1995.
- [28] *Landolt-Börnstein, Cryst. Solid State Phys.*, in: H. Ullmaier (Ed.), *Atomic Point Defects in Metals*, vol. 25, Springer Verlag, Berlin, 1991.
- [29] I.A. Schwirtlich, H. Schultz, *Philos. Mag. A* 42 (1980) 601–605.
- [30] A.S. Nowick, B.S. Berry, *Anelastic Relaxation in Crystalline Solids*, Academic Press, New York, 1972.
- [31] F. Povolò, B.J. Molinas, *Il Nuovo Cimento* 14 (1992) 287–332.
- [32] J.N. Lomer, J.F.R. Richardson, *J. Phys. C2* (32) (1972) 169–172.
- [33] O.A. Lambri, G.I. Zelada-Lambri, G.J. Cuello, P.B. Bozzano, J.A. García, *J. Nucl. Mater.* 385 (2009) 552–558.